THE JOURNAL OF BIOLOGICAL CHEMISTRY Vol. 279, No. 43, Issue of October 22, pp. 44775–44784, 2004

Printed in U.S.A.

Increased Site 1 Affinity Improves Biopotency of Porcine Growth Hormone

EVIDENCE AGAINST DIFFUSION DEPENDENT RECEPTOR DIMERIZATION*

Received for publication, June 2, 2004, and in revised form, August 4, 2004
Published, JBC Papers in Press, August 5, 2004, DOI 10.1074/jbc.M406092200

Yu Wan, Andrew McDevitt, Bojiang Shen, Mark L. Smythe, and Michael J. Waters‡

From the Institute for Molecular Bioscience and School of Biomedical Sciences, University of Queensland, St. Lucia 4072, Australia

Based on phage display optimization studies with human growth hormone (GH), it is thought that the biopotency of GH cannot be increased. This is proposed to be a result of the affinity of the first receptor for hormone far exceeding that which is required to trap the hormone long enough to allow diffusion of the second receptor to form the ternary complex, which initiates signaling. We report here that despite similar site 1 kinetics to the hGH/hGH receptor interaction, the potency of porcine GH for its receptor can be increased up to 5-fold by substituting hGH residues involved in site 1 binding into pGH. Based on extensive mutations and BIAcore studies, we show that the higher potency and site 1 affinity of hGH for the pGHR is primarily a result of a decreased off-rate associated with residues in the extended loop between helices 1 and 2 that interact with the two key tryptophans Trp^{104} and Trp^{169} in the receptor binding hot spot. Our mutagenic analysis has also identified a second determinant (Lys^{165}), which in addition to His^{169}, restricts the ability of non-primate hormones to activate hGH receptor. The increased biopotency of GH that we observe can be explained by a model for GH receptor activation where subunit alignment is critical for effective signaling.

The growth hormone receptor (GHR)[1] was the first class 1 cytokine receptor to be characterized, and the interaction between the human receptor and its ligand has been particularly well characterized (1, 2). The GHR has served as a paradigm for the ligand-induced dimerization mechanism that is believed to result in the activation of paired Janus kinases bound to the membrane proximal box 1 sequence of the receptor by a process of transphosphorylation. In the case of the GHR, JAK2 is the proximal effector, and once activated, it phosphorylates selected tyrosines in the receptor cytoplasmic domain, providing docking sites for SH2-domain containing signaling proteins and adaptors. Several important pathways are activated by this process, including the STAT5a/b, the ERK, and Akt pathways (3).

In a series of elegant investigations, a Genentech group demonstrated that the 4-helix bundle hormone possesses two non-identical binding surfaces, but binds to similar receptor binding sites in an ordered sequence, with the initial binding site possessing a higher affinity (site 1). Site 2 binding is stabilized by a further inter-receptor interaction involving the "dimerization domain" in the lower of the two cytokine homology modules (4–6). Both site 1 and site 2 interactions are critically dependent on a key tryptophan contributed by the upper cytokine module (Trp^{104}), with a second precisely oriented tryptophan (Trp^{169}) from the lower module also contributing critically to site 1 binding (2, 7). These tryptophans form the center of a hydrophobic binding surface (hot spot), which is the basis for the hormone-receptor interaction, with surrounding residues packing around these tryptophans to ensure high affinity interactions with the relevant hormone residues. Systematic mutagenesis has shown that essentially, the minihelix and loop between helices 1 and 2, together with residues in the center of helix 4 comprise the first hormone binding site 1 (1, 2). Residues at the amino terminus of the first helix and helix 3 comprise the second and smaller binding site on the hormone (5, 6).

Simulation of the process of bivalent hormone-dependent dimerization of receptor subunits shows that increasing site 1 affinity will shift the dose-response curve leftwards, whereas increasing site 2 affinity increases the maximum response (8, 9). The Genentech group therefore sought to increase the potency of human GH by increasing the affinity of both site 1 and site 2 for the receptor using phage display. However, despite a 400-fold increase in site 1 affinity, or a 40-fold increase in site 2 affinity, no increase in potency of hGH was observed in a cell proliferation assay (10). This led these workers to conclude that hGH is evolutionarily "optimized," because site 1 affinity in particular was sufficient to trap the hormone at the cell surface long enough for efficient dimerization with the second receptor subunit following its diffusion in the plane of the membrane to the receptor 1-hormone complex. This optimization is evidently very effective, because it was necessary to lower site 1 affinity by around 100-fold to observe a significant increase in the EC_{50} for cell proliferation (10).

While developing a cell proliferation assay for porcine GH based on stable expression of the pGH receptor, we noted that the biopotency of human GH was 5-fold greater than that of pGH. In an effort to understand the mechanisms responsible for this difference, and to create higher potency pGH analogues with economic potential, we have substituted site 1 binding residues from hGH residues into pGH. This also allowed us to identify species-specific determinants for hGH binding. We find that, contrary to hGH, it is possible to improve the biopotency of pGH, both by increasing on-rate and by decreasing off-rate constants. Our observations are consistent with a model for GH

* This work was supported by grants from the National Health and Medical Research Council (Australia) and the Australian Research Council. The costs of publication of this article were defrayed in part by the payment of page charges. This article must therefore be hereby marked "*advertisement*" in accordance with 18 U.S.C. Section 1734 solely to indicate this fact.

‡ To whom correspondence should be addressed. Tel.: 61-7-3346-2037; Fax: 61-7-3346-2101; E-mail: m.waters@imb.uq.edu.au.

[1] The abbreviations used are: GHR, growth hormone receptor; STAT, signal transducers and activators of transcription; ERK, extracellular signal-regulated kinase; GHBP, growth hormone-binding protein; RU, refractive index unit; WT, wild type; hGHR, human growth hormone receptor; pGH, porcine growth hormone; ECD, extracellular domain.

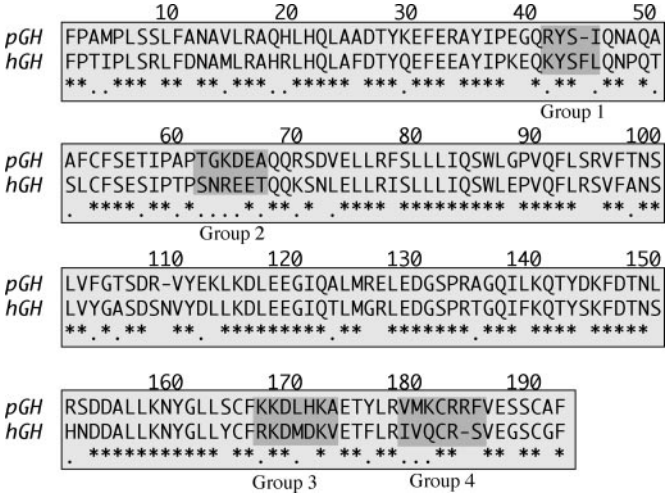

FIG. 1. **Comparison of human GH site 1 binding residues with equivalent porcine GH residues.** The site 1 binding residues were divided into four groups (highlighted): group 1, R41K/Insert44F/I45L; group 2, T61S/G62N/K63R/D64E/A66T; group 3, K165R/L168M/H169D/A171V; and group 4, V177I/M178V/K179Q/del R182/F183S.

receptor activation that involves a hormone-induced conformational change within a constitutive dimer, rather than hormone-induced receptor dimerization. Such a model has been proposed recently based on FRET and BRET data, and the ability to create constitutively active receptors independent of hormone by relative rotation of receptor subunits.[2]

EXPERIMENTAL PROCEDURES

Hormones

Recombinant hGH was obtained from the National Institute for Biological Standards and Control, Herts, UK, and interleukin-3 was a generous gift of Andrew Hapel, Australian National University, Canberra, Australia.

Mutagenesis

Gene Splicing by Overlap Extension mutagenesis (12) was employed to construct four cluster mutants based on the sequence comparison shown in Fig. 1, where residues in site 1 of hGH and the equivalent residues in pGH are highlighted. The primers listed below were used for the mutagenesis of the target residues R41K/Insert44F/I45L in group 1 (G1), T62S/G63N/K64R/D65E/A67T in group 2 (G2), K165R/L168M/H169D/A172V in group 3 (G3), and V178I/M179V/K180Q/del.183R/F184S in group 4 (G4). Each mutation is indicated in bold type, and the overlap regions are underlined. The primers are: PGH-a-For: 5′-GGATAACAATTTCACACAGGAGG-3′; G1–1b-Rev: 5′-TG**CAGGAA**GGAGTACTTCTGTCCCTCCGGGATG-3′; G1–1c-For: 5′-CAGA**AGTACTCCTTCC**TGCAGAACGCCCAGGCTG-3′; G2–1b-Rev: 5′-G**TCTCTT**CCA**GGTTGC**TGGGGGTCGGGATGGTCTC-3′; G2–1c-For: 5′-CA**GCAACAG**GGAAGAGA**C**CCAGCAGAGATCGGACG-3′; G3–1b-Rev: 5′-TGTCTCA**ACCTTGTC**CA**T**GTCCTTC**CT**GAAGCAGG-3′; G3–1c-For: 5′-TG**GACAAGGTT**GAGACATTCCTGCGGGTCATGAAG-3′; G4–3b-Rev: 5′-**CT—GCGACACTG**CA**C**GA**T**CCGCAGGTATGTCTCAGC-3′; G4–3c-For: 5′-G**ATCG**TG**C**AGTGTCGC—**AG**CGTGGAGAGCAGCTGTG-3′; and PGH-d-Rev: 5′-CCGCCAAAACAGCCAAGCTTGC-3′. Two separate fragments containing mutated bases were amplified from the pGH-pEC611 template by PCR using high fidelity thermostable polymerase, Pfu (Stratagene, La Jolla, CA). The first fragment was amplified with primers a and b. Primer b introduces a sequence change at the 3′ end of the PCR product. The second fragment was amplified with primers c and d, with primer c introducing the same mutation, but in the 5′ end of the PCR product. These two products share a segment of identical sequence, the overlap region. When these intermediate products are mixed, melted, and re-annealed, the two complementary mutant sequences generated from separate PCR anneal, facilitating overlap extension by DNA polymerase. This allows the creation of full-length pGH mutant DNA during the subsequent PCR with primers a and d.

Site-directed mutagenesis was carried out as described by QuikChange (Stratagene) to create a series of individual pGH mutants within the four groups described above. The following primers were used, where mutated bases are bolded and underlined. The primers are: G1–3For (R42K): 5′-TCCCGGAGGGACAGA**A**GTACTCCATCCAGAACG-3′; G1–3Rev (R42K): 5′-CGTTCTGGATGGAGTAC**T**TCTGTCCCTCCGGGA-3′ G1–4For (45F/I46L): 5′-GACAGAGGTACTCC**TTCCTG**CAGAACGCCCAGGCTG-3′; G1–4For (45F/I46L): 5′-CAGCCTGGGCGTTCTG**CAGGAA**GGAGTACCTCTGTC-3′; G2–2For (T62S/G63N): 5′-CCATCCCGGCCCCA**GCAA**CAAGGACGAGGCCCAG-3′; G2–2Rev (T62S/G63N): 5′-CTGGGCCTCGTCCTTG**TTGC**TGGGGGCCGGGATGG-3′; G2–4For (K64R/D65E): 5′-GCCCCCACGGGCA**GGGAA**GAGGCCCAGCAGAGATC-3′; G2–4Rev (K64R/D65E): 5′-GATCTCTGCTGGGCCTC**TTCCC**TGCCCGTGGGGGC-3′; G2–5For (A67T): 5′-ACGGGCAAGGACGAG**A**CCCAGCAGAGATCGG-3′; G2–5Rev (A67T): 5′-CCGATCTCTGCTGGG**T**CTCGTCCTTGCCCGT-3′; G3–1For (K165R): 5′-CTGCTCTCCTGCTTCA**G**GAAGGACCTGCACAAG-3′; G3–1Rev (K165R): 5′-CTTGTGCAGGTCCTTC**C**TGAAGCAGGAGAGCAG-3′; G4–1For (V177I): 5′-GAGACATACCTGCGG**A**TCATGAAGTGTCGCCG-3′; G4–1Rev (V177I): 5′-CGGCGACACTTCATGA**T**CCGCAGGTATGTCTC-3′; G4–2For (V177I/M178V/K179Q): 5′-GACATACCTGCGG**A**TC**G**TG**C**AGTGTCGCCGCTTCG-3′; G4–2Rev (V177I/M178VK179/Q): 5′-CGAAGCGGCGACACT**G**CA**C**GA**T**CCGCAGGTATGTC-3′; G4–6For (F184S): 5′-CATGAAGTGTCGCCGC**AG**CGTGGAGAGCAGCTGTG-3′; G4–6Rev (F184S): 5′-CACAGCTGCTCTCCACG**CT**GCGGCGACACTTCATG-3′; G4–7For (del.R183/F184S): 5′-CATGAAGTGTCGC—**AG**CGTGGAGAGCAGCTGTG-3′; G4–7Rev (del.R183/F184S): 5′-CACAGCTGCTCTCCACG**CT**—GCGACACTTCATG-3′.

GHBP Mutations

To facilitate bacterial expression of pGHBP, a number of third bases in the wild type pGHBP DNA were mutated to the preferred bacterial codons, where the mammalian codon was only rarely used in *Escherichia coli*. There were codons 21 (GGG to GGT), 25 (ACA to ACC), 28 (GTC to GTG), 29 (CTT to CTG), 30 (GTC to GTG), 31 (AGA to CGT), 38 (AGA to CGT), and 174 (AGA to CGT). In addition, to facilitate coupling to the BIAcore chip, pGHBP(S201C), pGHBP(S237C), and hGHBP(S201C) were prepared by site-directed mutagenesis from pGHBP and hGHBP cDNAs in pCDNA3.1(+) with the following primers. The mutated bases corresponding to amino acid substitutions are bolded and underlined. The primers are: S219C-pGHBP-For: 5′-CAGTTCCGGTGTAC**TGC**TTGAGACTG GATAAAG-3′; S219C-pGHBP-Rev: 5′-CTTTATCCAGTCTCAAG**C**AGTACACCGGAACTG-3′; S237C-pGHBP-For: 5′-CACTTCCTCAGATG**TGCTAATAAGCTT**GTGAAGAAG-3′; S237C-pGHBP-Rev:5′-CTTCTTCAC**AAGCTT**ATTAGC**A**CATCTGAGGAAGTG3′; S219C-hGHBP-For: 5′-CATCAGTTCCAGTGTACT**GC**TTGAAAGTGGATAAG-3′; S219C-hGHBP-Rev: 5′-CTTATCCACTTTCAA**GC**AGTACACTGGAACTGATG-3′.

Expression Constructs

Expression in *E. coli* also required the removal of the mammalian signal sequence. This was achieved by introducing an NdeI site and a START codon (ATG) at the 5′ end and a STOP codon (TAA) and a HindIII site at the 3′ end of the pGH, pGHBP, and hGHBP sequences in pCE611(pGH), pCDNA3.1(pGHBP), and pCDNA3.1(hGHBP). The following primers were used to achieve this by site-directed mutagenesis. The restriction sites are bolded and underlined, and start and stop codons are in italics: pGH-For: 5′-GAAACAG**CATA*TG***TTCCCAGCCATGCCGC-3′; pGH-Rev: 5′-CAGCC**AAGCTT*CTA***TGCCTGCAGGTCGACTC-3′; PGHBP-For: 5′-CAGGCTCA**CAT*ATG***GCTTTTTCTGGGAGTGAAGCC-3′; pGHBP-Rev: 5′-TTCAC**AAGCTT**A*TTA*AGCTCATCTGAGGAAGTGTTAC-3′; hGHBP-For: 5′-CAGGCTCA**CAT*ATG***TTTTCTGGAAGTGAGGCC-3′; hGHBP-Rev: 5′-TTCAC**AAGCTT**-A*TTA*GCTCATCTGAGGAAGTGTTAC-3′.

After each mutation was confirmed by autosequencing using the ABI Prism big dye terminator version 3.0 (Australian Genome Research Facility), the mutant cDNAs were digested with the relevant restriction enzymes such that the mutated region was excised. The pET-20b(+) expression vector (catalog number 69739-3, Novagen, Madison, WI) was also cut with the same enzymes followed by ligation of the mutant DNA segment. The mutant cDNA segments in the expression vector were again sequenced between the subcloning sites to eliminate any spurious mutations.

Expression and Purification of Recombinant Proteins

pGH and pGH Mutants—All constructs were transformed into *E. coli* strain BL21(DE3), and isolated colonies from agar plates were grown in

[2] R. J. Brown, J. J. Adams, R. A. Pelakanos, Y. Wan, W. J. McKinstry, K. Palethorpe, R. M. Seeber, T. A. Monks, K. A. Eidne, M. W. Parker, and M. J. Waters, unpublished data.

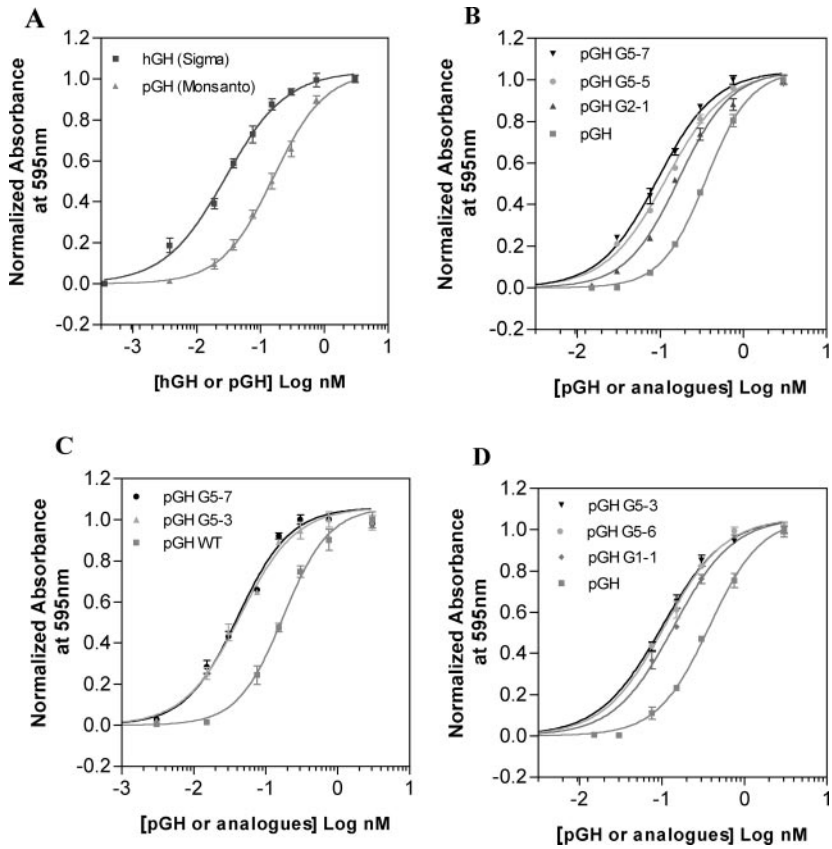

FIG. 2. **Representative curves showing proliferative response of BaF/B03 cells expressing pGH receptor to hGH, pGH wild type (*A*), and pGH analogues with higher potency (*B–D*).** Cell proliferation was assessed using the 3-(4,5-dimethylthiazol-2-yl)-2,5-diphenyltetrazolium bromide assay (see "Experimental Procedures"). The *points on the curves* represent normalized absorbance values (mean ± S.E.) from the data of duplicate experiments with each trial consisting of triplicate runs. *P.Mut.G1-1* represents mutant 1 of porcine GH group 1, and the others are similarly indicated.

3-ml cultures, then induced with 1 mM isopropyl-1-thio-β-D-galactopyranoside. The clones expressing the highest level of recombinant proteins were selected by PAGE using Coomassie Blue and used immediately for protein expression.

Selected bacterial clones expressing pGH and pGH mutants were used to initiate fermentation by inoculation in 50 ml of LB medium at 37 °C, followed by an overnight culture at 15 °C. This culture was then diluted into 500 ml of TB medium and grown in 2 × 2-liter flasks at 37 °C to an A_{600} of 0.7–0.9. Isopropyl-1-thio-β-D-galactopyranoside was then added to 1 mM. Growth was continued for an additional 3–4 h to A_{600} of 1.5–1.6, after which the cells were pelleted for 10 min at 6,000 × *g*, re-suspended in 20 ml of cold water containing 0.2 mM phenylmethylsulfonyl fluoride, and stored at −70 °C for less than 2 weeks. For preparation of inclusion bodies, frozen precipitate was thawed and the cells were lysed by passage twice through a French Press at 1000 p.s.i. The lysate was washed by centrifuging sequentially with 100 ml of cold water, 100 ml of washing buffer 1 (1 M NaCl, 25 mM Na_3BO_3, pH 9.0), and 100 ml of washing buffer 2 (phosphate-buffered saline containing 1 M urea and 1% Triton X-100, pH 7.8). In each case the pellets were resuspended by gentle homogenization with a Polytron, and the suspension was centrifuged at 10,000 × *g* for 12 min at 4 °C. SDS-PAGE (not shown) revealed that the molecular weight of the recombinant protein was identical to pGH wild type.

The inclusion body pellets were then re-suspended in 10 ml of denaturation buffer (10 mM glycine, 10 mM dithiothreitol, 40 mM sodium borate, pH 9.1), 4 volumes of 6 M guanidine HCl was added, and the ixture was stirred for 1 h. After this, the suspension was centrifuged and the supernatant was diluted with 5 volumes of 4 M urea, 1 mM glycine, 25 mM Na_3BO_3 (pH 9.1), such that the refolding was initiated, and this was facilitated by agitating gently to allow air oxidation, for 5 h at 4 °C. Oxidation was followed by dialysis against 8 liters of 1 M urea, 25 mM Na_3BO_3 (pH 9.1) and 2× 8 liters of 25 mM Na_3BO_3 (pH 9.1) for 36 h at 4 °C.

The refolded oxidized protein was then loaded onto a Q-Sepharose (catalog number 17051010, Amersham Biosciences) column (1.6 × 20 cm) pre-equilibrated with 25 mM Na_3BO_3 (pH 9.1) at 4 °C. Elution was carried out with a continuous NaCl gradient (0–1 M) in the equilibration buffer at 2 ml/min, and 5-ml fractions were collected. Protein concentration was determined by absorbance at 280 nm, and monomer content was determined by 14% SDS-PAGE in the absence of reducing agents. Gels were stained with Coomassie Blue R-250. Fractions judged to be greater than 95% pure monomer were selected for further analysis.

pGHBP and hGHBP—Recombinant porcine GHBP WT, pGHBP(S201C), and pGHBP(S237C) were expressed in *E. coli* BL21(DE3) and purified as described in Wan *et al.* (13). Wild type hGHBP and hGHB(S201C) cDNA coding sequence for residues 1–237 was ligated into the pET20b(+) vector and transformed into *E. coli*, BL21 CodonPlus(DE3)-RIL (catalog number 230245, Stratagene) according to the instruction manual (revision 050004). Subsequent expression and purification of these proteins was as described in Wan *et al.* (13). Radioligand binding of purified GHBPs was according to Ref. 14.

Surface Plasmon Resonance

All kinetic experiments were carried out on a BIAcore 3000 instrument (BIAcore AB, Uppsala, Sweden) at 25 °C. pGHbp and hGHbp were immobilized on Sensor Chips SA (BR-1000–32, BIAcore AB) and changes in refractive index upon binding of hormone were used for kinetic measurements.

Preparation of Sensor Chips—To immobilize pGHBP and hGHBP in discrete orientations on the BIAcore sensor chip SA (streptavidin), a cysteine residue was introduced at Ser^{201} or Ser^{237} as previously described (1). In our hands, direct coupling of the free thiol to the sensor chip inactivated the binding protein. Therefore the free thiols were conjugated with Biotin-BMCC (Pierce) to form a mixed disulfide, with excess Biotin-BMCC being removed with a PD-10 desalting column (Amersham Biosciences). After preconditioning sensor chips with three consecutive 1-min injections of 1 M NaCl in 50 mM NaOH, biotinylated GHBPs were immobilized onto the streptavidin at the chip surface until ~140 RUs (refractive index unit) were immobilized. This was achieved by injecting biotinylated GHBPs (2 × 5 μl of 1 μg/1 ml in 10 mM sodium acetate, pH 6.0, buffer) over the chip surface following the BIAcore protocol. The pGHBP(S201C) and pGHBP(S237C) were immobilized on the surfaces of flow cells 2 and 4, respectively, and flow cells 1 and 3 were used as reference for on-line reference subtraction. After immobilization, maximum binding capacity was determined by saturating the biosensor with 240 nM pGH or hGH.

Analyses of Binding Kinetics—Association rates were calculated from binding profiles obtained by injecting increasing concentrations of each GH analogue. In all cases, 25 μl of 0.5, 3.75, 7.5, 15, 30, and 60 nM

analogue were injected. Each concentration of the analyte was run three times over the surface of the GHBP Chip at a flow rate of 5 μl/min. Injection time was 5 min, stabilization time was 1 min, and dissociation time was 5 min. High salt buffer-EP was used to prevent long-range electrostatic effects and to mimic physiological ionic strength, and non-specific binding was reduced by including 0.02% Tween 20. The surface was regenerated by washed for 30 s with 25 μl of 4.5 M $MgCl_2$. Control experiments showed that this was sufficient to remove all the bound hormone and that the surface could be reused more than 100 times without significant change in the binding kinetics.

Association and dissociation kinetic constants were calculated by BIAevaluation 3.2 software using a simple 1:1 Langmuir model. A wild type reference was always included to control for any chip variation.

TABLE I

Biopotency values for pGH mutants and hGH relative to pGH

The values shown in this table are means ± S.E.

Ligands	Mutated residues	EC_{50} relative to PGH wild type
PGH WT		1.00
HGH WT		0.19 ± 0.02[a]
G1 (1)	R41K/Ins.44F/I45L	0.31 ± 0.01[a]
G1 (3)	R41K	0.87 ± 0.02
G1 (4)	Ins.44F/I45L	0.50 ± 0.03[b]
G2 (1)	T61S/G62N/K63R/D64E/A66T	0.36 ± 0.03[b]
G2 (2)	T61S/G62N	1.17 ± 0.06
G2 (4)	K63R/D64E	1.94 ± 0.06[b]
G2 (5)	A66T	0.65 ± 0.08
G4 (2)	V177I/M178V/K179Q	1.15 ± 0.00
G4 (3)	V177I/M178V/K179Q/del.182R/F183S	0.60 ± 0.03
G4 (6)	F183S	0.46 ± 0.01[b]
G4 (7)	Del.182R/F183S	0.35 ± 0.03[b]
G5 (1)	G1(1) + G2(2)	0.38 ± 0.01[b]
G5 (2)	G1(1) + G2(4)	0.85 ± 0.07
G5 (3)	G1(1) + G4(7)	0.22 ± 0.01[a]
G5 (4)	G2(1) + G4(7)	0.26 ± 0.03[a]
G5 (5)	G2(1) + G1(4)	0.24 ± 0.01[a]
G5 (6)	G1(1) + G4(7) + G2(5)	0.22 ± 0.01[a]
G5 (7)	G2(1) + G4(7) + G1(4)	0.20 ± 0.01[a]

[a] $p < 0.01$ relative to pGH.
[b] $p < 0.05$ relative to pGH.

The concentration of the hGH, pGH, and analogues were determined by absorbance at 280 nm and BCA analysis.

Cell Proliferation Assays

The interleukin-3-dependent cell line, BAF/B03, stably transfected with full-length pGHR or human GH receptor (hGHR) was used for cell proliferation assays (15). Both lines express around 6000 receptors/cell at the cell surface by Scatchard analysis. Cells were maintained in RPMI 1640 media with 10% Serum Supreme (a fetal bovine serum alternative supplied by BioWhittaker) and 5 mM hGH. In preparation for the assay, 80% confluent BAF/B03 cells were washed with phosphate-buffered saline, re-suspended in assay buffer (RPMI 1640 with 1% serum supreme, without hGH), and incubated for 12–14 h. Cells were then pelleted, washed with phosphate-buffered saline, and re-suspended to 6×10^5 cells/ml in assay buffer. 50 μl of cell suspension was added to each well of a 96-well microtiter plate. This was followed by 100 μl of pGH or pGH mutants (at 8 different concentrations: 100, 25, 10, 5, 2.5, 0.625, and 0.1 ng/ml) to each of triplicate wells. Cells were then incubated for 36–40 h at 37 °C, after which 3-(4,5-dimethylthiazol-2-yl)-2,5-diphenyltetrazolium bromide was used to determine cell viability and number as described previously (15). Curve fitting was performed using Prism 3 and derived EC_{50} values were compared by analysis of variance. Each mutant was assayed three times, and the mean values are reported.

Homology Modeling

Protein Data Bank structures 1HWG, 3HHR, and 1A22 were used as templates for constructing a model of pGH/pGHBP, with pGH and pGHBP protein sequences being obtained from NCBI. Sequences were read into InsightII (Accelrys, San Diego, CA) and aligned using structurally conserved regions within the homology module. For pGH and pGHBP, 10 structures were built using the modeler function with a high level of refinement. The structures were minimized using Discover3 and the CFF91 forcefield. Model structures were scored with a combination of ProCheck, ProStat, and Verify, and also assessed visually. Models of the highest affinity mutants were also created using the Biopolymer module. The pGH-pGHBP complex model was created using 3HHR as a template. pGH and pGHBP were superimposed onto 3HHR to check for bumps. These were removed by manual rotation of torsions. The complex was then minimized, and analyzed by ProCheck and compared with 3HHR. This process was then performed for mutant structures.

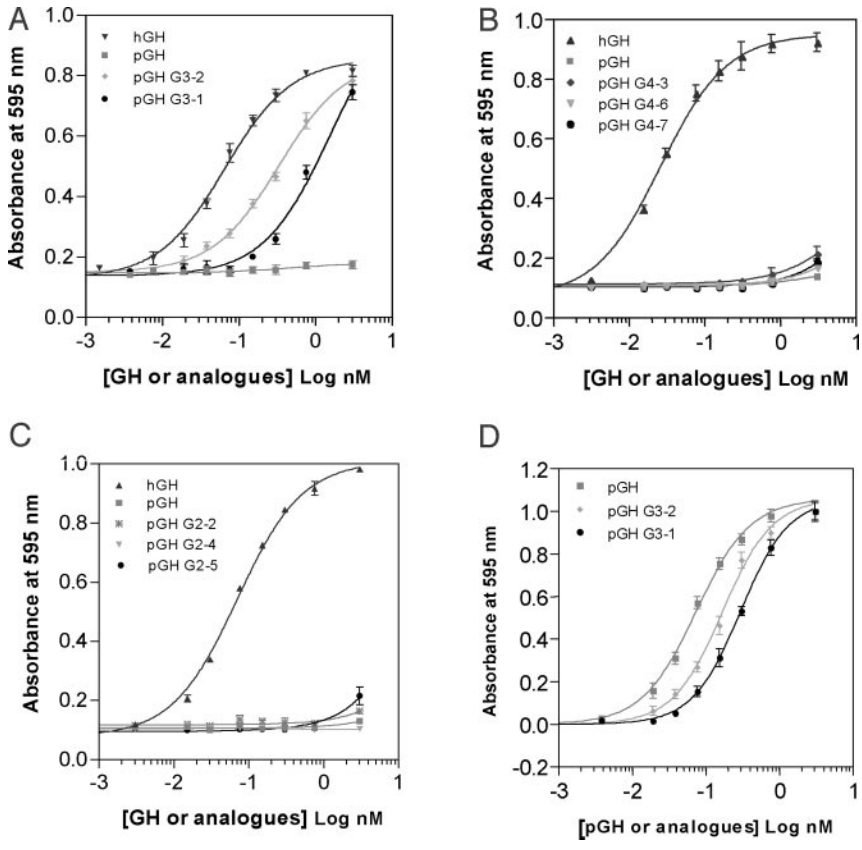

FIG. 3. **Proliferative response of BaF/B03 cells expressing hGH receptor (*panels A–C*) and pGH receptor (*panel D*) to hGH, pGH, and pGH analogues.** pGH G3-1 consists of L168M/H169D/A171V and G3-2 comprises K165R/L168M/H169D/A171V. Cell proliferation was assessed using the 3-(4,5-dimethylthiazol-2-yl)-2,5-diphenyltetrazolium bromide assay (see "Experimental Procedures"). The *points on the curves* represent absorbance values (mean ± S.E.).

TABLE II

Proliferative ability of pGH mutants relative to hGH and pGH wild type

The values shown in this table represent mean ± S.E.

Receptor	Ligands	Mutated residues	EC_{50} relative to pGH wild type
hGHR	PGH		NR
	HGH		1.00
	G3(1)	L168M/H169D/A171V	19.4 ± 1.26[a]
	G3(2)	K165R/L168M/H169D/A171V	5.38 ± 0.15[a]
	G2(1)	T61S/G62N/K63R/D64E/A66T	NR[c]
	G2(5)	A66T	NR
pGHR	PGH WT		1.00
	G3(1)	L168M/H169D/A171V	3.05 ± 0.20[b]
	G3(2)	K165R/L168M/H169D/A171V	2.28 ± 0.21[b]

[a] $p < 0.01$ relative to GH wild type.
[b] $p < 0.05$ relative to GH wild type.
[c] NR, no response.

TABLE III

Kinetic data for binding of WT growth hormones to GHBPs immobilized on BIAcore sensor chip SA

1000 RU = 1.0 ng/mm^2. Stoichiometry of binding were calculated according to the following formula: $(RU_{Max}(GH))/(RU\ (GHBP)) \times$ (Mr. GHBP)/(Mr.GH).

Hormone	Matrix	Stoichiometry (pGH:pGHBP)	K_{on}	K_{off}	K_D
			$s^{-1}\ M^{-1}$		*nM*
pGH WT	pGHBP (S201C)	0.89:1	3.4 E + 5	6.1 E−4	1.80
pGH WT	pGHBP (S237C)	0.47:1	5.1 E + 5	1.6 E−4	0.30
hGH WT	hGHBP (S201C)	0.87:1	3.2 E + 5	3.9 E−4	1.22

TABLE IV

Relative on-rates, off-rates, and affinities for pGH mutants and hGH to pGHbp(S201C) immobilized on the SA-matrix of BIAcore biosensor

The relative change in on-rate was calculated from K_{on} Mut/K_{on} WT and off-rate from K_{off} Mut/K_{off}WT. The change in K_D was calculated as $[K_{off}/K_{on}$ (Mut)]/$[K_{off}/K_{on}$ (WT)] and K_A from $1/K_D$. The values of R_{max} were calculated from R_{max} Mut/R_{max} WT. The $\Delta\Delta G$ values were calculated as +RT Ln K_D.

Ligands	Residues by mutagenesis	Changes in kinetics (Mut/WT)					
		On-rate	Off-rate	K_A	K_D	R_{max}	$\Delta\Delta G$
							Kcal/mol
PGH		1.00	1.00	1.00	1.00	1.00	0.00
HGH		0.73	0.08	9.34	0.11	1.17	−1.32
G1(1)	R41K/Ins.44F/I45L	1.57	0.79	1.98	0.52	1.22	−0.39
G1(3)	R41K	1.13	1.05	1.03	0.94	1.10	−0.04
G1(4)	Ins.44F/I45L	1.22	0.63	1.94	0.51	1.29	−0.40
G2(1)	T61S/G62N/K63R/D64E/A66T	1.17	0.05	23.8	0.04	1.24	−1.87
G2(2)	T61S/G62N	0.77	0.98	0.80	1.16	1.06	+0.09
G2(4)	K63R/D64E	0.89	1.92	0.49	2.13	0.69	+0.45
G2(5)	A66T	0.77	0.42	1.85	0.53	1.14	−0.37
G4(3)	V177I/M178V/K179Q/del.182R/F183S	0.86	1.43	0.60	1.67	1.05	+0.30
G4(6)	F183S	1.29	0.90	1.41	0.70	1.09	−0.21
G4(7)	Del. 182R/F183S	1.21	0.82	1.43	0.70	1.27	−0.23
G5(1)	G1(1) + G2(2)	1.15	0.53	2.19	0.45	1.26	−0.46
G5(2)	G1(1) + G2(4)	1.85	2.62	0.71	1.39	0.91	+0.20
G5(3)	G1(1) + G4(7)	1.51	0.90	1.67	0.61	1.44	−0.30
G5(4)	G2(1) + G4(7)	1.28	0.07	18.0	0.05	1.33	−1.70
G5(5)	G2(1) + G1(4)	1.29	0.06	21.7	0.05	1.31	−1.82
G5(6)	G1(1) + G4(7) + G2(5)	1.51	0.52	2.78	0.35	1.43	−0.62
G5(7)	G2(1) + G4(7) + G1(4)	1.66	0.08	20.4	0.05	1.45	−1.80

Molecular Dynamics

Molecular dynamic simulations were performed in the Discover3 module of InsightII. Minimized pGH and pGH-Group 1 were equilibrated at 300 K, before generating 50 structures using 2000 fs of molecular dynamic. The structures were analyzed in the DeCipher module of InsightII, to assess the mobility of the minihelix. Mobility was measured as the distance between 3 residues located on the same side of the helix.

RESULTS

Biopotency of Analogues in a pGH Receptor-based Assay—The 5-fold biopotency difference that prompted this study is shown in Fig. 2*A*, which compares the potencies of hGH and pGH against the pGH receptor in the BaF cell assay. To address the basis for this difference, we expressed and purified 20 pGH analogues each possessing different combinations of the key binding elements of hGH identified for site 1 binding to receptor 1 (1). This resulted in 4 groups of mutants, corresponding to the minihelix between helices 1 and 2 (G1), R41K/Inserted 44F/I45L; the extended loop between helices 1 and 2 (G2), T61S/G62N/K63R/D64E/A66T; the central part of helix 4 (G3), K165R/L168M/H169D/A171V; and the carboxyl-terminal end of helix 4 (G4), V177I/M178V/K179Q/del.182R/F183S (Fig. 1). Variants with individual mutations in each group were also created. The biopotency curves for several of these are shown in Fig. 2, *B–D*, and the EC_{50} values are listed in Table I.

Of the four groups of pGH analogues, the most significant reduction in EC_{50} for cell proliferation were for group 1 (1), R41K/Inserted 44F/I45L; group 2 (1), T61S/G62N/K63R/D64E/A66T; and group 4 (7), del.182R/F183S. There were no biopotency-improved variants in group 3. Interestingly, although neither double nor single mutations showed any significant reduction in the EC_{50} in group 2, the sum of all mutations in

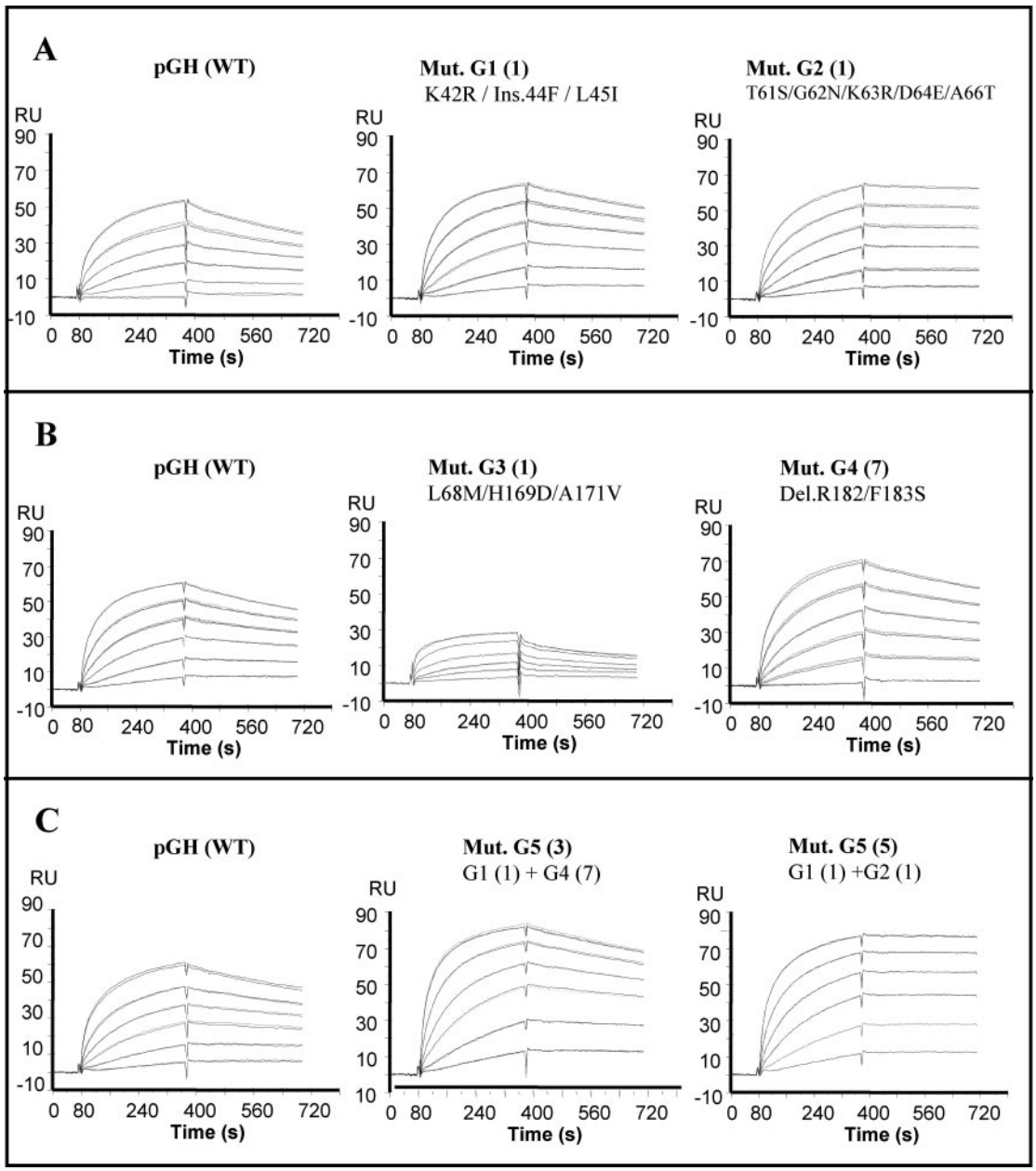

FIG. 4. **Representative sensorgrams showing association and dissociation kinetics for pGH wild type and mutants binding with pGHBP.** The simulated sensorgrams from simultaneous and global fit of the experimental data are shown superimposed upon the experimental sensorgrams. All sensorgrams were from pGHBP(S201C) on the SA Biosensor Chip after injections of serial dilutions of pGH wild type and pGH mutants at 60, 30, 15, 7.5, 3.75, and 0.5 nM. *A*, injection of pGH mutants group 1-1 (G1(1)) and group 2-1 (G2(1)); *B*, injection of pGH mutants groups 3-1 (G3(1)) and 4-7 (G4(7)); *C*, injections of the combinations of affinity improved pGH mutants.

this group showed a highly significant improvement (0.36 ± 0.028) in EC_{50} relative to pGH WT.

To further improve pGH analogue biopotency, the biopotency-improved variants in groups 1, 2, and 4 were combined into group 5 (G5). As seen in Table I, most of the combination mutants in G5 showed that higher biopotency was achieved by the approach, except for G5 (2) where residues decreasing biopotency (K63R/D64E) were included.

The most significant improvement in biopotency was seen with the combined analogues G5(3), G5(5), G5(6), and G5(7), which had 4.6-, 4.1-, 4.5-, and 5.1-fold increases in biopotency, respectively, compared with pGH WT (Table I and Fig. 2). The greatest biopotency-improved analogue, G5(7), consisted of 10 mutations: R41K/Inserted 44F/I45L/T61S/G62N/K63R/D64E/A66T/del.182R/F183S. However, a mutant with only 5 residue changes (G5(3)) possessed a biopotency very close to that of G5 (7).

For regulatory reasons, it was important to determine whether these increased biopotency pGH mutants cross-react with the hGH receptor. Analysis with the BAF/B03 cell line expressing hGHR revealed that pGH wild type could not activate the hGHR up to 50 nM and this was the case for all pGH analogues except for group 3 analogues and, to a minor extent, for group 5 (7). This is illustrated in Fig. 3 and Table II, which show that pGH mutant G3(1) L168M/H169D/A171V has a 19-fold lower potency for hGH receptor than hGH itself, and mutant G3(2) K165R/L168M/H169D/A171V reaches one-fifth the potency of hGH. However, these mutants are 2–3-fold less potent than pGH in the pGH receptor-based cell bioassay. To understand the basis for the differences in biopotency observed with these hybrid pGH mutants, we undertook biosensor analysis for binding kinetics with immobilized pGHR extracellular domain (ECD or GHBP).

TABLE V

Relative on-rates, off-rates, and affinities for pGH mutants and hGH to pGHbp(S237C) immobilized on the SA-matrix of BIAcore biosensor

The relative change in on-rate was calculated from K_{on} Mut/K_{on} WT and off-rate from K_{off} Mut/K_{off}WT. The change in K_D was calculated as [K_{off}/K_{on} (Mut)]/[K_{off}/K_{on} (WT)] and K_A from 1/K_D. The values of R_{max} were calculated from R_{max} Mut/R_{max} WT.

Ligands	Residues by mutagenesis	Changes in kinetics (Mut/WT)				
		On-rate	Off-rate	K_A	K_D	R_{max}
PGH		1.00	1.00	1.00	1.00	1.00
HGH		0.80	0.05	16.0	0.06	1.11
G1(1)	R41K/Ins.44F/I45L	1.28	0.69	1.81	0.55	1.16
G1(3)	R41K	1.12	1.25	0.89	1.11	1.01
G1(4)	Ins.44F/I45L	1.08	1.13	0.97	1.04	1.06
G2(1)	T61S/G62N/K63R/D64E/A66T	1.10	0.27	4.18	0.24	1.18
G2(2)	T61S/G62N	0.91	0.82	1.10	0.90	1.00
G2(4)	K63R/D64E	0.89	1.24	0.75	1.34	0.85
G2(5)	A66T	0.88	0.82	1.10	0.93	1.08
G4(3)	V177I/M178V/K179Q/del.182R/F183S	0.90	1.00	0.90	1.08	1.02
G4(6)	F183S	1.26	0.81	1.56	0.66	1.04
G4(7)	Del.182R/F183S	1.26	0.78	1.56	0.62	1.17
G5(1)	G1(1) + G2(2)	1.16	0.75	1.52	0.67	1.16
G5(2)	G1(1) + G2(4)	1.45	1.94	0.73	1.37	1.02
G5(3)	G1(1) + G4(7)	1.38	1.11	1.14	0.89	1.28
G5(4)	G2(1) + G4(7)	1.21	0.77	1.56	0.61	1.11
G5(5)	G2(1) + G1(4)	1.04	0.40	2.48	0.40	1.24
G5(6)	G1(1) + G4(7) + G2(5)	1.54	1.25	1.25	0.75	1.27
G5(7)	G2(1) + G4(7) + G1(4)	1.40	0.94	1.50	0.63	1.27

Kinetic Parameters—Two GHR ECD orientations were used for these studies, based on studies with the hGHR ECD (1). In this case, immobilization through S201C prevents dimer formation between ECDs, and yields site 1 kinetic parameters, whereas immobilization through S237C allows hormone-induced dimer formation, and provides an overall measure of complex formation similar to binding to intact receptor at the cell surface. This is verified for the pGHR ECD in Table III, which shows that the maximum binding stoichiometry for pGH binding to S201C immobilized ECD approached 1.0, whereas the stoichiometry for S237C ECD was close to 0.5. It is notable that the absolute values for off- and on-rate constants do not differ markedly between pGH and hGH binding to their respective ECDs. The calculated K_D values (Table III) are similar to the values reported by the Genentech group (1), indicating that the purified ECDs were correctly refolded and immobilized.

Binding parameters for site 1 using the S201C pGHR ECD are presented in Table IV and representative sensorgrams in Fig. 4. hGH is seen to have a marginally lower on-rate that WT pGH. It can be seen that only the minihelix substitution R41K/Insert44F/I45L significantly increases the on-rate constant, and this is largely a result of substitution of Lys for Arg at position 41. This substitution essentially doubled the affinity constant. In support of this conclusion, combination mutants with the minihelix substitution also show an increased on-rate, except when decreased by another mutation.

Analysis of off-rates was more revealing (Table IV). The off-rate for hGH binding to S201C pGHR ECD is 12.5 times slower than for pGH, and this accounts for the 9-fold higher affinity of hGH for the pGHR ECD. This decreased off-rate appears to be a result of residues in the extended loop between helices 1 and 2, because substitution of only these 5 hGH residues into pGH produces a comparable decrease in off-rate constant as seen with hGH itself. Interestingly, with the exception of A66T, none of the individual or paired substitutions in this sequence was able to decrease the off-rate. Evidently the entire 5-residue substitution is required, and this is confirmed in the combination mutants. This difference in the off-rate is sufficient to increase the affinity constant by over 20-fold, exceeding that of hGH itself.

Analysis of the 20 mutants with the S237C pGHR ECD chip was also revealing (Table V). In all cases the on-rate constant was greater than the corresponding S201C pGHR ECD value, although the effect was less than 2-fold. The off-rate constants with hGH and most of the pGH mutants are less than the value with S201C pGHR EC, presumably as a result of the stabilization associated with formation of the ternary complex. However, this is not the case for mutants involving the extended loop between helices 1 and 2, either alone or in combination with other mutations. Evidently the stabilization of site 1 binding that results from substitution of the 5 extended loop residues is sharply decreased on formation of the ternary complex.

Primate Specificity Determinants—The basis for increased biopotency of Group 3 fourth helix substituents seen in the hGH receptor-based cell bioassay was investigated using a S201C hGHR ECD sensor chip. As shown in Table VI, the on-rate constant was the critical factor in determining affinity. Previously (15) we showed that His^{169} is the key primate specificity determinant, and this was verified here. In addition, the K165R substitution was able to further increase the on-rate constant by a factor of nearly 3-fold. This allowed the mutant pGH to bind to hGH receptor site 1 with an affinity exceeding one-tenth that of wild type hGH, similar to its one-fifth biopotency in the cell assay.

Relationship between Kinetic Parameters and Biopotency—As illustrated in Fig. 5, across the 20 pGH mutants there is a linear relationship between normalized site 1 biopotency and the normalized site 1 dissociation constant, obtained with the S201C pGHR ECD chip. This linear relationship also applies for the S237C pGHR ECD chip. This relationship is not seen with hGH (10).

DISCUSSION

This study has shown that, in contrast to hGH (10), pGH is not "evolutionarily optimized," and can be mutated to improve its biopotency. Indeed, there is a linear relationship between site 1 affinity of pGH and biopotency over a 10-fold range. This accords with the predictions of Illondo *et al.* (8) and Matthews *et al.* (9) for hormone-induced dimerization of a cytokine receptor. However, the finding that a 400-fold increase in site 1 affinity for hGH or a 40-fold increase in affinity for site 2, did not result in any increased biopotency led Pearce *et al.* (10) to examine these predictions more closely, and to propose that the limiting factor in receptor activation was diffusion of the second receptor to the hormone-receptor 1 complex. They argued that because site 1 affinity needed to be *reduced* over 50-fold to see

TABLE VI

Relative on-rates, off-rates, and affinities for pGH mutants binding to hGHBP and pGHBP immobilized on the SA-matrix of BIAcore biosensor

The relative change in on-rate was calculated from K_{on} Mut/K_{on} WT and off-rate from K_{off} Mut/ K_{off}WT. The change in K_D was calculated as [K_{off}/K_{on} (Mut)]/[K_{off}/K_{on} (WT)] and K_A from $1/K_D$. The values of R_{max} were calculated from R_{max} Mut/R_{max} WT. Absolute values for wt pGH and hGH are given in parentheses: Values for mutants are relative to WT that are normalized to 1.0.

GHR	Ligand	Residues by mutagenesis	Changes in kinetics (Mut/WT)				
			On-rate	Off-rate	K_A	K_D	R_{max}
			1/ms	*1/s*	*1/M*	*M*	*RU*
	HGH		1 (1.9^5)	1 (3.5^{-4})	1 (5.5^8)	1 (1.8^{-9})	1 (43)
	pGH		NB	NB	NB	NB	NB
hGHBP(S201C)	G3(1)	L168M/H169D/A171V	0.08	2.41	0.03	29.6	0.24
	G3(2)	K165R/L168M/H169D/A171V	0.23	2.22	0.11	9.60	0.43
	G2(1)	T61S/G62N/K63R/D64E/A66T	NB[a]	NB	NB	NB	NB
	G2(2)	T61S/G62N	NB	NB	NB	NB	NB
	G2(4)	K63R/D64E	NB	NB	NB	NB	NB
	G2(5)	A66T	NB	NB	NB	NB	NB
	pGH		1 (1.8^5)	1 (6.8^{-4})	1 (2.7^8)	1 (3.7^{-9})	1 (38)
pGHBP(S201C)	G3(1)	L168M/H169D/A171V	1.06	1.62	0.63	1.57	0.63
	G3(2)	K165R/L168M/H169D/A171V	1.31	1.09	1.18	0.85	1.06
	pGH		1 (2.3^5)	1 (2.5^{-4})	1 (9.2^8)	1 (1.1^{-9})	1 (42)
pGHBP(S237C)	G3(1)	L168M/H169D/A171V	1.48	1.28	1.15	0.86	0.72
	G3(2)	K165R/L168M/H169D/A171V	1.52	1.04	1.46	0.67	0.92

[a] NB, no binding.

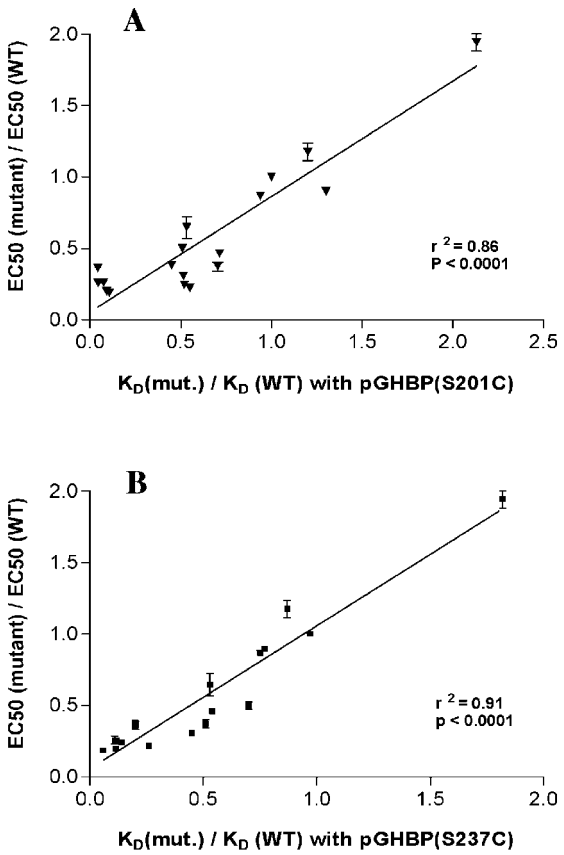

FIG. 5. **Relationship between biopotency and kinetics of porcine GH analogues.** *A* shows EC_{50} mutant/EC_{50} wild type *versus* the K_D mutant/K_D wild type with pGHBP(S201C). *B* shows binding with pGHBP(S237C) on sensor chip SA. The values for Biopotency and kinetics are shown in Tables I and III, respectively, except for the data from group 3. Correlation with K_{off} was weaker, for both S201C GHBP (r^2 = 0.44) and S237C GHBP (r^2 = 0.21).

a decrease in biopotency, the binding to site 1 far exceeds the requirement to immobilize the hormone until the second receptor formed the active ternary complex. A comprehensive set of calculations accounting for membrane diffusion rates during the receptor dimerization process showed that, based on the dimerization model and a conservative estimate of cell diameter and receptor density, no change in hormone biopotency was possible unless the affinity was reduced at least 20-fold. However, our BIAcore analysis shows that site 1 affinity of pGH for its receptor is only slightly less than that of hGH for its receptor site, yet we find a linear relationship between site 1 affinity and biopotency for pGH, so the diffusion limited argument does not appear to apply.

An alternative explanation is that the phage display-matured hGH binds in a less signaling competent manner to its receptor than the wild type hormone. It is clear from the crystallography study of Schiffer *et al.* (16) that phage display mutations alter the way that site 1 binds to its receptor, but what was surprising in this study was that site 2 interactions are also very different in the crystal structure, even though the mutations were introduced exclusively in site 1. We find, conversely, that site 2 and dimerization domain interactions can alter site 1 interactions, as exemplified by the decrease in affinity with S237C pGHR ECD (which detects ternary complex formation) when high affinity mutants involving the extended loop between helices 1 and 2 (site 1) are examined. In this case alone, the affinity for the S237C pGHR ECD chip is lower than the affinity for the S201C chip, implying that site 2 and inter-receptor interactions destabilize site 1 interactions. This is presumably a result of disturbing the packing around the key hydrophobic binding hotspot that involves the two tryptophans, Trp^{104} and Trp^{169} (2). The loss of overall (S237C) affinity we observe in this case may contribute to preventing a further increase in biopotency beyond the 5-fold wild type, even though the site 1 affinity increase is over 20-fold.

In the simple hormone-induced receptor dimerization model, the manner in which the receptor subunits bind to the hormone is of little relevance. However, we have recently proposed a new model for GH receptor activation that is based on relative rotation of subunits within a pre-existing receptor dimer.[2] In this model, relative orientation of receptor subunits is critical for effective signaling, as has been shown for the homologous erythropoietin receptor (17). We suggest that the reason that the phage display variants of hGH were unable to improve

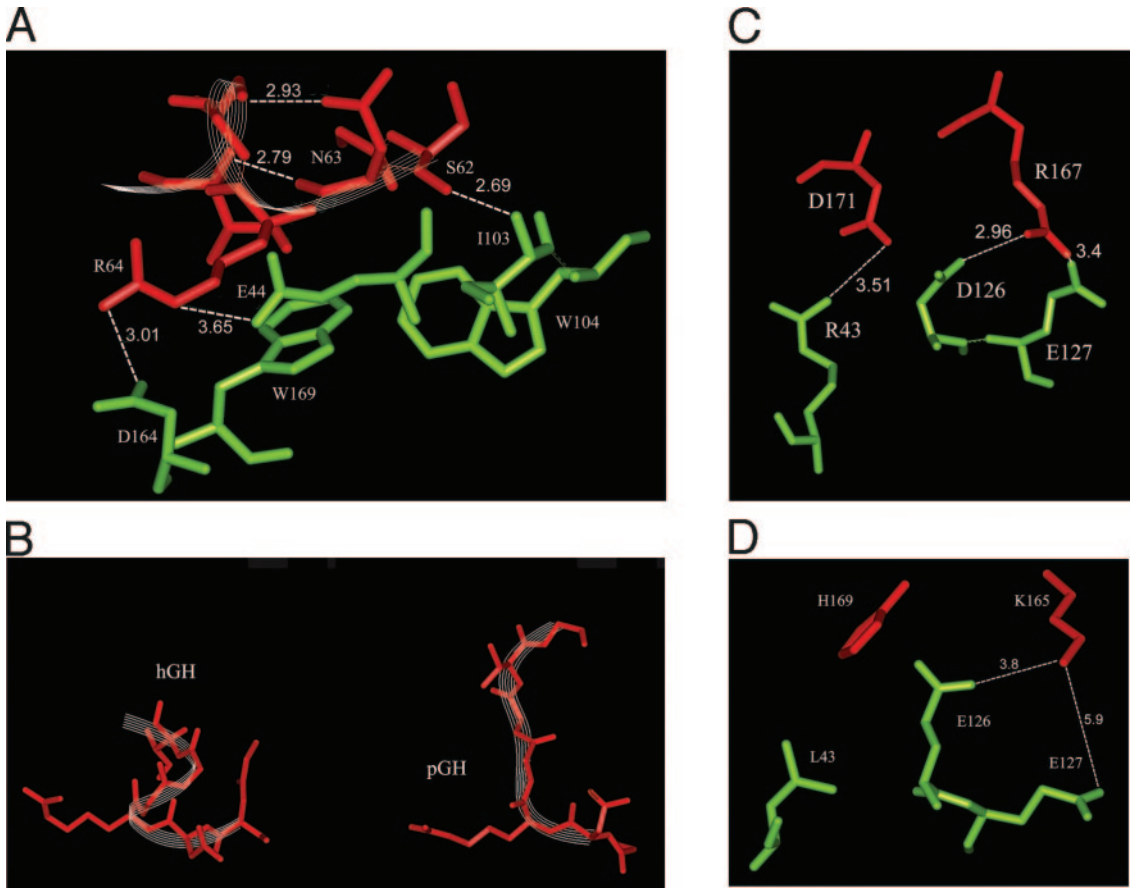

FIG. 6. *A*, hGH/hGH receptor crystal structure (Protein Data Bank codes 1HWG and 3HHR) showing extended loop residues (Group 2) of hGH, their packing with the key two tryptophans of receptor 1, and their hydrogen bonds/ionic interactions with the receptor. Also shown as a *white ribbon* is the ASX motif positioned by two hydrogen bonds, which confers rigidity to this loop and stabilizes interactions around the hydrophobic core. Distances are shown in angstroms. *B*, comparison of the ASX motif in the hGH extended loop with conformation of homologous pGH loop residues, derived from the homology model. Note the absence of two key hydrogen bonds in pGH prevents formation of the stabilized ASX motif. *C*, key residues conferring primate species specificity in the hGH/hGHR crystal structure, and *D*, comparison with equivalent residues in the pGH homology model.

biopotency is that they caused misalignment of receptor subunits in some way, which resulted in a lower proportion of occupied receptors initiating their response at a given hormone concentration. In this view, the pGH mutants identified here were able to act more efficiently, because they preserve the framework needed for signaling-competent alignment of receptor subunits, which is present in hGH.

We have undertaken homology modeling and molecular dynamics studies to understand the bases for the changes in site 1 kinetics that we observe with our mutants. Our homology model for the pGH receptor, based on the human structures, shows that the substitutions influencing on-rate (R41K/Insert44F/I45L) in the minihelix between helices 1 and 2 can be explained by two effects. The first is an improvement in the minihelix structure and stability as a result of insertion of the Phe, evident in molecular dynamics simulations that show greater mobility of the wild type minihelix. The second contributing factor appears to be the ability of human Lys^{41} to form a productive salt bridge with Glu^{127} of the receptor, where Arg^{41} of pGH forms only a hydrogen bond to receptor Cys^{122}.

The reduction in off-rate associated with the group of 5 substitutions in the extended loop between helices 1 and 2 (T61S/G62N/K63R/D64E/A66T) most likely relates to their role in packing around the important tryptophans Trp^{104} (hGH Ser^{62}) and Trp^{169} (hGH Arg^{64}), which are known to determine the off-rate (1). There are also additional bonds that are predicted to be present with the introduced human sequence that are absent with WT pGH (see Fig. 6). Thus, human Arg^{64} forms an ionic bond with receptor Asp^{164}, and an ionic bond with Glu^{44}, whereas porcine Lys^{63} is able to form only an ionic bond to Asp^{164}. Arg^{64} packs closely with receptor Trp^{169}, so its positioning is important. In addition, the carbonyl of hGH Ser^{62} forms a hydrogen bond to the amide of receptor Ile^{103}, which is important in positioning receptor Trp^{104}. Another important factor is likely to be the ability of carbonyl of the side chain of Asn^{63} of hGH (Gly in pGH) to form a hydrogen bond with the backbone amide of hGH Glu^{66}, which acts to stabilize the loop (referred to as an ASX motif (18)). Moreover, the backbone carbonyl of Asn^{63} hydrogen bonds to the hydroxyl side chain of Thr^{67} (Ala in pGH). These stabilizing hydrogen bonds are likely to influence the positioning of human Arg^{64}, which forms important contacts with receptor Trp^{169}.

An analysis of sequences from different species, together with the original alanine scanning study of Cunningham *et al.* (19) and the crystal structure of the 2:1 complex, led Sousa *et al.* (20) to show that Asp^{171} of hGH (His in non-primate GH) is the primary determinant responsible for the inability of non-primate GH to activate the human receptor. We subsequently analyzed this in detail, with both receptor and hormone substitutions and modeling studies, showing the incompatibility of His^{169} of pGH opposite the primate receptor Arg^{43} (15). Here we independently confirm our earlier conclusions about Asp^{171}-His^{169}, and also find that a further substitution of primate Arg (*i.e.* Arg^{167} of hGH) at Lys^{165} results in a pGH mutant that is able to activate the human receptor with only 5-fold lower

potency than hGH itself. This is confirmed with kinetic analysis, which shows that the Arg substitution at Lys^{165} increases the on-rate a further 4-fold. As shown in Fig. 6, this appears to be a result of altered interactions with key electrostatic contributors to binding in the linker region between cytokine homology modules (Asp^{126} and Glu^{127}). It can be seen in the N-η1 and N-η2 of Arg^{167} in the hGH hydrogen bond/salt bridge to the O-ϵ1 of Glu^{127} hGHR (5). This Arg is also sufficiently close to the carboxy1 group of Glu^{126} to form a productive salt bridge (4.3 Å). In the case of pGH, Lys^{165} also hydrogen bonds to Glu^{127}, but cannot form the additional salt bridge to Glu^{126}. This appears to be the only additional bond that can be formed with hGH, and its absence could explain the 3-fold loss of site 1 affinity and 4-fold loss in biopotency seen against the hGHR. However, this loss of affinity is not seen in the homologous pGH-pGHR interaction, because the longer Glu^{126} side chain of pGH allows electrostatic interaction with Lys^{165} of pGH, and His^{169} could also form a weak ionic interaction with Glu^{126}.

Our report of the creation of higher potency cytokine analogues is not unique, although we have been unable to find any literature reports of protein engineering that has resulted in significantly higher potency class 1 cytokine analogues. Okabe *et al.* (21) reported that the *in vitro* potency granulocyte colony-stimulating factor could be increased up to 4-fold by 5 substitutions identified from a screen of about 100 mutations. Generally, cytokine potency has otherwise been increased *in vivo* by PEGylation (*e.g.* tumor necrosis factor-α (22)), altered glycosylation (*e.g.* granulocyte colony-stimulating factor (23) and erythropoietin (24)), removal of residues responsible for binding to a competing binding protein (*e.g.* insulin-like growth factor-1 (25)), or by making a fusion protein with another bioactive protein (interleukin-3 (11)). In these cases the increased biopotency results mainly from prolonged half-life.

In conclusion, in contrast to human GH, it has been possible to engineer higher potency analogues of porcine GH by increasing site 1 affinity, and this may apply for other non-primate hormones. The finding that there is an essentially linear relationship between site 1 affinity and biopotency has important implications for understanding the process of growth hormone receptor activation.

Acknowledgments—We thank Gary Shooter and Richard Brown for valuable discussions.

REFERENCES

1. Cunningham, B. C., and Wells, J. A. (1993) *J. Mol. Biol.* **234,** 554–563
2. Clackson, T., Ultsch, M. H., Wells, J. A., and de Vos, A. M. (1998) *J. Mol. Biol.* **277,** 1111–1128
3. Argetsinger, L. S., and Carter-Su, C. (1996) *Physiol. Rev.* **76,** 1089–1107
4. Cunningham, B. C., Ultsch, M., de Vos, A. M., Mulkerrin, M. G., Clauser, K. R., and Wells, J. A. (1991) *Science* **254,** 821–825
5. De Vos, A. M., Ultsch, M., and Kossiakoff, A. A. (1992) *Science* **255,** 306–312
6. Chen, C., Brinkworth, R., and Waters, M. J. (1997) *J. Biol. Chem.* **272,** 5133–5140
7. Bernat, B., Pal, G., Sun, M., and Kossiakoff, A. A. (2003) *Proc. Natl. Acad. Sci. U. S. A.* **100,** 952–957
8. Ilondo, M., Damholt, A. B., Cunningham, B. C., Wells, J. A., De Meyts, P., and Shymko, R. M. (1994) *Endocrinology* **134,** 2397–2403
9. Matthews, D. J., Topping, R. S., Cass, R. T., and Giebel, L. B. (1996) *Proc. Natl. Acad. Sci. U. S. A.* **93,** 9471–9476
10. Pearce, K. H., Cunningham, B. C., Fuh, G., Teeri, T., and Wells, J. A. (1999) *Biochemistry* **38,** 81–89
11. Difalco, M. R., and Congote, L. F. (1997) *Biochem. J.* **326,** 407–413
12. Horton, R. M., Ho, S. N., Pullen, J. K., Hunt, H. D., Cai, Z., and Pease, L. R. (1993) *Methods Enzymol.* **217,** 270–279
13. Wan, Y., Zheng, Y. Z., Harris, J. M., Brown, R., and Waters, M. J. (2003) *Mol. Endocrinol.* **17,** 2240–2250
14. Barnard, R., Bundesen, P. G., Rylatt, D. B., and Waters, M. J. (1985) *Biochem. J.* **231,** 459–468
15. Behncken, S. N., Rowlinson, S. W., Rowland, J. E., Conway-Campbell, B. L., Monks, T. A., and Waters, M. J. (1997) *J. Biol. Chem.* **272,** 27077–27083
16. Schiffer, C., Ultsch, M., Walsh, S., Somers, W., de Vos, A. M., and Kossiakoff, A. (2002) *J. Mol. Biol.* **316,** 277–289
17. Syed, R. S., Reid, S. W., Li, C., Cheetham, J. C., Aoki, K. H., Liu, B., Zhan, H., Osslund, T. D., Chirino, A. J., Zhang, J., Finer-Moore, J., Elliott, S., Sitney, K., Katz, B. A., Matthews, D. J., Wendoloski, J. J., Egrie, J., and Stroud, R. M. (1998) *Nature* **395,** 511–516
18. Wan, W. Y., and Milner-White, E. J. (1999) *J. Mol. Biol.* **286,** 1633–1649
19. Cunningham, B. C., Jhurani, P., Ng, P., and Wells, J. A. (1989) *Science* **243,** 1330–1336
20. Sousa, S. C., Frick, G. P., Yip, R., Lobo, R. B., Tai, L. R., and Goodman, H. M. (1995) *Proc. Natl. Acad. Sci. U. S. A.* **92,** 959–963
21. Okabe, M., Asano, M., Kuga, T., Komatsu, Y., Yamasaki, M., Yokoo, Y., Itoh, S., Morimoto, M., and Oka, T. (1990) *Blood* **75,** 1788–1793
22. Yamamoto, Y., Tsutsumi, Y., Yoshioka, Y., Nishibata, T., Kobayashi, K., Okamoto, T., Mukai, Y., Shimizu, T., Nakagawa, S., Nagata, S., and Mayumi, T. (2003) *Nat. Biotechnol.* **21,** 546–552
23. Nissen, C. (1994) *Eur. J. Cancer* **30,** Suppl. 3**,** S12–S14
24. Egrie, J. C., Dwyer, E., Browne, J. K., Hitz, A., and Lykos, M. A. (2003) *Exp. Hematol.* **31,** 290–299
25. Simes, J. M., Wallace, J. C., and Walton, P. E. (1991) *J. Endocrinol.* **130,** 93–99

Increased Site 1 Affinity Improves Biopotency of Porcine Growth Hormone: EVIDENCE AGAINST DIFFUSION DEPENDENT RECEPTOR DIMERIZATION

Yu Wan, Andrew McDevitt, Bojiang Shen, Mark L. Smythe and Michael J. Waters

J. Biol. Chem. 2004, 279:44775-44784.
doi: 10.1074/jbc.M406092200 originally published online August 5, 2004
